Effect of deformable mirror sequence on performance of multiconjugate adaptive optics

Marcos Alejandro van Dam, Bruno Femenia Castella, Yolanda Martin Hernando, Miguel Nunez Cagigal, Luzma Montoya, Dirk Schmidt, Francois Rigaut, Guido Agapito

AO4ELT7 - June 2023 - Avignon

Effect of deformable mirror sequence on performance of multiconjugate adaptive optics

Marcos A. van Dam[a], Bruno Femenía Castellá[b], Yolanda Martín Hernando[c,d], Miguel Núñez Cagigal[c,d], Luzma M. Montoya[c,d], Dirk Schmidt[e], François Rigaut[f], and Guido Agapito[g]

[a]Flat Wavefronts, 21 Lascelles Street, Christchurch 8022, New Zealand
[b]DLR, Münchner Str. 20, 82234 Wessling, Germany
[c]Instituto de Astrofísica de Canarias, C/ Vía Láctea S/N, E-38200 La Laguna, Spain
[d]Departamento de Astrofísica, Universidad de La Laguna, E-38205 La Laguna, Tenerife, Spain
[e]National Solar Observatory, 3665 Discovery Drive, Boulder, CO 80303, USA
[f]Advanced Instrumentation and Technology Centre, Research School of Astronomy and Astrophysics, the Australian National University, Mount Stromlo Observatory, Weston ACT 2611, Australia
[g]INAF — Osservatorio Astrofisico di Arcetri, Firenze, Italy

ABSTRACT

Multi-conjugate adaptive optics (MCAO) uses two or more deformable mirrors (DMs) at conjugate altitudes approximately matched to the atmospheric turbulence layers to increase the corrected field of view. An important unresolved problem for MCAO is determining the optimal sequence of the DMs. Some theoretical considerations and numerical studies suggest that ordering the DMs from lowest to highest altitude reduces the effects of scintillation, while on-sky experiments report that the best performance is attained with the ground-layer DM placed last. Using analytical calculations and numerical experiments with Fresnel propagation of Kolmogorov turbulence, we demonstrate that the scintillation results from spatial frequencies higher than the spatial sampling of high-altitude DMs are able to correct. Hence, the effect of scintillation is not impacted by MCAO correction regardless of the sequence of the DMs. Using end-to-end numerical simulations, we find that the dynamic misregistration between the DMs and the wavefront sensors is minimized by placing the ground-layer DM last,

Send correspondence to Marcos van Dam, e-mail: marcos@flatwavefronts.com

leading to increased loop stability and lower wavefront errors. Contrary to conventional wisdom, we recommend that the DMs be sequenced from highest to lowest altitude.

Keywords: adaptive optics, multiconjugate adaptive optics, scintillation, Fresnel propagation, dynamic misregistration

1. INTRODUCTION

In classical adaptive optics (AO) systems, a single deformable mirror (DM) optically conjugated to the pupil corrects for wavefront aberrations caused by atmospheric turbulence. The wavefront correction is best in the direction in which it is sensed but degrades with increasing angular distance from the guide star, a phenomenon called angular anisoplanatism. Angular anisoplanatism results from the fact that the guide star senses a different portion of the mid- and high-altitude turbulence layers than the science target and restricts the useful science field of view to between $5''$ to $30''$, depending on science wavelength and the site. At longer wavelengths, the tolerance on wavefront errors is larger and a larger field of view can be used. The corrected science field of view can be expanded by adding one or more additional DMs to correct for mid- and high-altitude turbulence layers in what is known as multiconjugate adaptive optics (MCAO).[1] MCAO expands the science field of view to typically $30''$ to $120''$, depending on the science wavelength.

MCAO has enjoyed some success in night-time astronomy, with the Multi-conjugate Adaptive optics Demonstrator (MAD)[2] at the Very Large Telescope (VLT) and the Gemini Multi-Conjugate Adaptive Optics System (GeMS)[3, 4] on Gemini South paving the way. GeMS was designed as a three DM system, but actually uses two DMs because of the failure of one of the DMs. It has been routinely producing corrected near infrared science images over an $85''\times85''$ field since 2013. The LINC-NIRVANA MCAO system is currently being deployed on the Large Binocular Telescope.[5] Solar MCAO has an even longer history.[6, 7, 8] The three-DM MCAO system Clear at the Goode Solar Telescope has been providing high-order AO correction over a $30''\times30''$ at visible wavelengths since 2016.[9] The next generation of MCAO systems is under design, including MAVIS[10] for the Very Large Telescope (VLT), an MCAO system on Daniel K. Inouye Solar Telescope (DKIST)[11] and an MCAO system for the European Solar Telescope (EST).[12] A vexing and unresolved issue in the design of the MCAO systems is selecting the sequence in which the incoming wavefront encounters the DMs.

For wide-field optical compensation, Hardy (1998) argues using geometric optics considerations that the correct approach is to place the DMs after the focal plane of the telescope and to correct from lowest altitude to highest altitude.[13] Using this sequence of DMs, it is theoretically possible to perfectly cancel the wavefront aberrations. Hardy claims that inverting the DM sequence "is unsuitable for multiple plane compensation because distortion in the intermediate layers spoils the conjugate imaging", but did not quantify this effect.

As an aberrated wave propagates to the ground, the aberrated phase leads to variations in the amplitude of the electric field as well as its phase. The variation in amplitude is known as scintillation and is experienced with the naked eye as the twinkling of stars. While both amplitude and phase variations degrade the image, phase variations dominate the degradation in image quality in astronomical observations. Flicker (2001) was the first to quantify the impact of the DM conjugation order on the Strehl ratio,[14] using an infinite aperture telescope and two DMs that perfectly cancel the wavefront aberrations originating from two discrete turbulence layers. This study concludes that the correcting from lowest to highest layers leads to a relative Strehl ratio improvement of the order of 10% to 15% depending on wavelength and zenith angle. Farley *et al.* (2017) extends the calculations by using a finite telescope diameter as well as a large number of turbulent layers and DMs, but still assuming perfect compensation of the turbulent layers.[15] The paper concludes that correcting the low-altitude layers first leads to a relative increase in Strehl ratio of up to 15% at 500 nm, with the difference due to increased scintillation. None of these studies considered the effect of the DM sequence on the performance of the WFS or the stability of the control loop.

The altitude layers are imaged by the telescope in the opposite order, from highest to lowest altitude. Reversing the order of the altitude layers requires the inclusion of relay optics between each DM,[13] leading to a reduction in optical throughput and an increase in thermal background, complexity and cost. For these practical reasons, GeMS and MAD place the DMs in decreasing order of conjugate altitude. Clear deliberately allows the insertion of a pupil plane DM before the other DMs in order to experiment with the DM sequence on-sky. An

on-sky experiment was recently performed using Clear that compared the image quality delivered by the MCAO system with the pupil plane DM placed first with the performance attained with the DM placed last.[16]

In a recently published paper, we demonstrate that the scintillation is caused by phase errors with a spatial frequency higher than it typically corrected by astronomical AO systems.[17] In this paper, we also show how the DM sequence can affect the registration between the DM and the wavefront sensors (WFSs). We use a new simulation tool called PropAO, which is described in van Dam *et al.*[17] PropAO uses the Python version of the PROPER Optical Simulation library to implement the Fresnel propagation and other operations.[18] The calls to NumPY functions were replaced by the equivalent CuPY functions in order to take advantage of GPU acceleration.

The remainder of the paper is distributed as follows. In Section 2, we describe the two mechanisms by which the DM sequence affects MCAO performance: scintillation and DM to WFS registration. Section 3 presents simulations used to reproduce and understand the on-sky results from Clear, while simulations in Section 4 demonstrate that the DM sequence in the MAVIS optical design is optimal. Conclusions are drawn in Section 5.

2. EFFECTS OF DM SEQUENCE ON PERFORMANCE OF MCAO

The DM sequence affects the MCAO performance in two different ways: the scintillation (Section 2.1) and the DM to WFS registration (Section 2.2).

2.1 Scintillation

Scintillation refers to the phenomenon whereby a phase aberration in a wave is converted into amplitude fluctuations as the wave propagates. The effect of the scintillation on the image quality is quantified via the log-amplitude variations. Previous papers[14, 15] have shown that by ordering the DMs from lowest altitude to highest altitude, the effect of scintillation can be compensated. However, we showed that the log-amplitude of the wave due to atmospheric turbulence is dominated by higher spatial frequencies than are corrected in astronomical AO systems.[17] In addition, the conjugate of the DMs need to be well matched to the height of the turbulence, which is not practical because the height of the turbulence and the zenith angle of the observation change with time.

2.2 DM to WFS dynamic misregistration

The DM sequence also affects the performance of the wavefront sensing and control loop, an important point which is not addressed by any of the previous studies. MCAO systems typically employ Shack-Hartmann wavefront sensors (SH WFSs) optically conjugate to the pupil plane. The registration between the DM actuators and the WFS is calibrated by poking DM actuators and measuring the response of the WFS. Any change in the surface of a high-altitude DM situated between the pupil plane DM and the WFSs leads to a change in registration between the pupil plane DM and the WFSs. Since the optical surface of the high-altitude DM changes with time, this phenomenon is referred to as dynamic misregistration.[19]

We can illustrate the DM to WFS dynamic misregistration as follows (Figure 1). Consider an fictitious MCAO system with two DMs. DM0 is conjugate to the pupil plane, while DM1 is conjugate to 10 km. Here, we show a Shack-Hartmann WFS matched to the DM in the Fried configuration, but this problem is common to all WFSs. If a DM0 actuator is poked, then the centroids are sensed symmetrically by all four neighboring subapertures. However, if a wavefront is applied to DM1, such as a tilt, then the registration between DM0 and the WFS changes. This leads to a reduction in performance and, for a sufficiently large wavefront on DM1, the loop can go unstable. Note that if DM1 is placed before DM0, then a wavefront on DM0 does not affect the registration between DM1 and the WFS, because DM0 is conjugate to the WFS.

Loop instability due to the dynamic misregistration effect has been seen in simulations, leading to worse than expected performance in strong turbulence.[20] We conclude that placing the pupil plane DM last is beneficial for solar MCAO systems, where the observations are often at low elevations and the WFS sampling is fine.

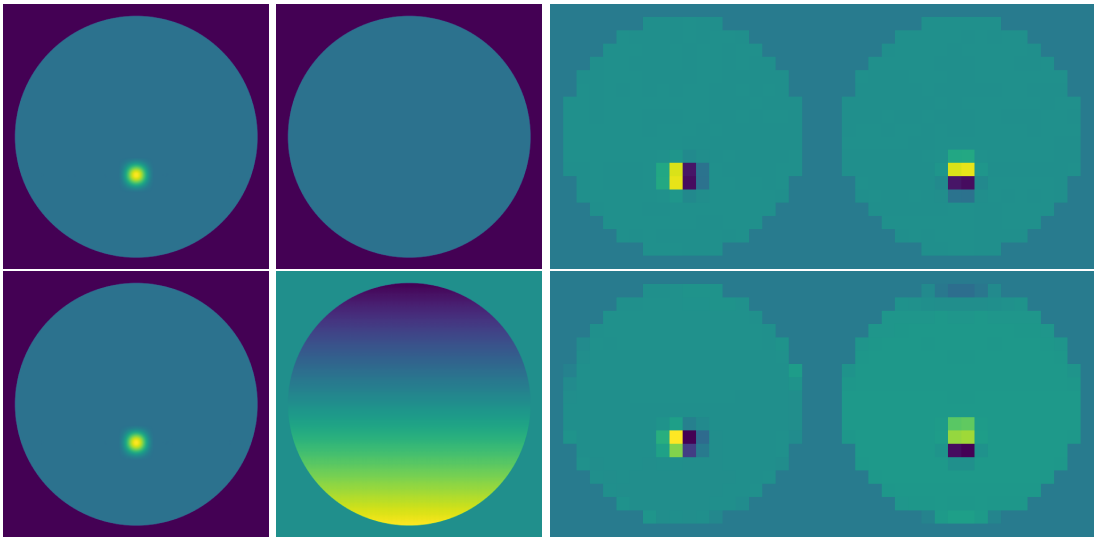

Figure 1: From left to right, the DM0 commands, the DM1 commands, and the measured tip-tilt removed x- and y-centroids. The top row shows a flat DM1, while the bottom row shows the results for a tilted DM1.

3. SIMULATIONS OF THE CLEAR MCAO SYSTEM

In this section, we present the simulation parameters and results of a numerical experiment to determine how the DM sequence affects the performance of the Clear MCAO system. The simulation aims to mimic the on-sky DM sequence experiment performed by Schmidt *et al.*[16]

3.1 Simulation parameters

The Goode Solar Telescope has a telescope diameter of 1.6 m, which is modeled as a circular pupil using 8 mm pixels. The zenith angle was 34° and the value of r_0 at 500 nm in the observing direction was 0.08 m. Other atmospheric parameters are tabulated in Table 1.

To quantify the scintillation, we consider the toy problem of an observation at zenith with the Fried parameter $r_0 = 0.08$ m at a wavelength of 500 nm. We adopt a turbulence profile with a vertical distribution of turbulence representative of the EST. The atmospheric parameters used are tabulated in Table 1.

Table 1: Turbulence profile used in the simulations of the Clear MCAO system.

Elevation (m)	0	1000	2000	4000	8000	16000
C_n^2 ($\times 10^{-14}\mathrm{m}^{1/3}$)	55.4	15.1	5.0	6.0	7.1	12.1
Turbulence fraction	0.55	0.15	0.05	0.06	0.07	0.12
Wind speed ($\mathrm{m\,s}^{-1}$)	5.6	6.25	7.57	13.31	19.06	12.14
Wind direction (°)	65	249	194	80	26	239

A regular grid of nine wavefront sensing directions taking the values of $-12''$, $0''$ and $12''$ is used to sense the wavefront. The wavefront sensing parameters are tabulated in Table 2.

Table 2: Wavefront sensing parameters.

Wavelength	525 nm
Subapertures across pupil	16
Subaperture size	88 mm
Wavefront sensing directions	$-12''$, $0''$, $12''$

The experiment on Clear had four DMs with characteristics described in Table 3, with only three DMs used at a time. The interactuator spacing for DM3 matches the size of the WFS subapertures and the location of the actuators corresponds to the corners of the subapertures in what is commonly known as the Fried configuration.[21]

Table 3: Deformable mirror parameters used to simulate the on-sky experiment at Clear. Note that DM3 was actually at 3000 m and not at 4000 m as described in Schmidt *et al.*[16]

DM	0	1	2	3
Altitude	0 m	8000 m	3000 m	0 m
Actuators	19×19	13×13	17×17	17×17
Actuator pitch	80 mm	336 mm	192 mm	88 mm

The following DM sequences were compared in simulation:

(A): DM0, DM1, DM2 at 0 m, 8000 m and 3000 m

(B): DM1, DM2, DM3 at 8000 m, 3000 m and 0 m

(C): DM3, DM2, DM1 at 0 m, 3000 m and 8000 m

(D): DM3, DM1, DM2 at 0 m, 8000 m and 3000 m

Sequences (A) and (D) correspond to the case where an adaptive secondary mirror is conjugate to the pupil plane and the remaining DMs are sequenced in the order in which they are imaged by the telescope. Sequence (B) has the DMs from highest to lowest altitude, while Sequence (C) has the DMs from lowest to highest altitude.

The reconstructor is a regularized least-squares reconstructor similar to the one described by van Dam *et al.*.[22] A closed-loop controller operating at a frame rate of 1500 Hz with a one frame loop delay is used. Each simulation consists of a total of 15000 iterations for an integration time of 10 s, and three sets of simulations were run for each sequence.

The Strehl ratio was evaluated at the same locations as the WFS but at a wavelength of 656 nm, which corresponds to Hα. We apply a 1.42 m diameter pupil stop in the science camera to emulate the on-sky experiment.

There are two significant differences between the simulations and the on-sky test by Schmidt *et al.*[16] First, the WFS used in the simulations is an ideal Shack-Hartmann WFS, where the noiseless centroid of a point source is used to define the wavefront slopes. In the Clear experiment, low-resolution images of a patch of the sun are correlated against a reference image. Second, Clear uses a modal reconstructor with Karhunen-Loeve modes, where the number of modes reconstructed implicitly defines the strength of the regularization. We did not attempt to replicate this reconstructor and used a zonal reconstructor instead.

3.2 Simulation results

The experiment on Clear rapidly alternated Sequences (A) and (B) while taking narrowband images on the science camera. The seeing was measured with an independent WFS located before the DMs.[16] The image contrast in the central region of the science camera was measured to be higher using Sequence (B) than Sequence (A) at all three wavelengths recorded in the experiment. For example, the contrast at Hα had a median value of 2.4% using Sequence (A) and 2.8% with Sequence (B).

The simulated average Strehl ratio as a function of position in the field is plotted in Figure 2. The Strehl ratio for Sequence (B) is higher than for Sequence (A), in agreement with the on-sky experiment. Although it is difficult to translate Strehl ratio into image contrast, it appears that the difference in performance was more significant for Clear than in the simulations. To understand how statistically significant the results in Figure 2, the 27 individual Strehl measurements (three simulations and nine positions on the science field) were plotted. Figure 3 shows the individual results from Sequences (B), (C) and (D) with the corresponding result from Sequence (A) subtracted. Sequence (B) is the only sequence with the pupil plane DM last. For this reason,

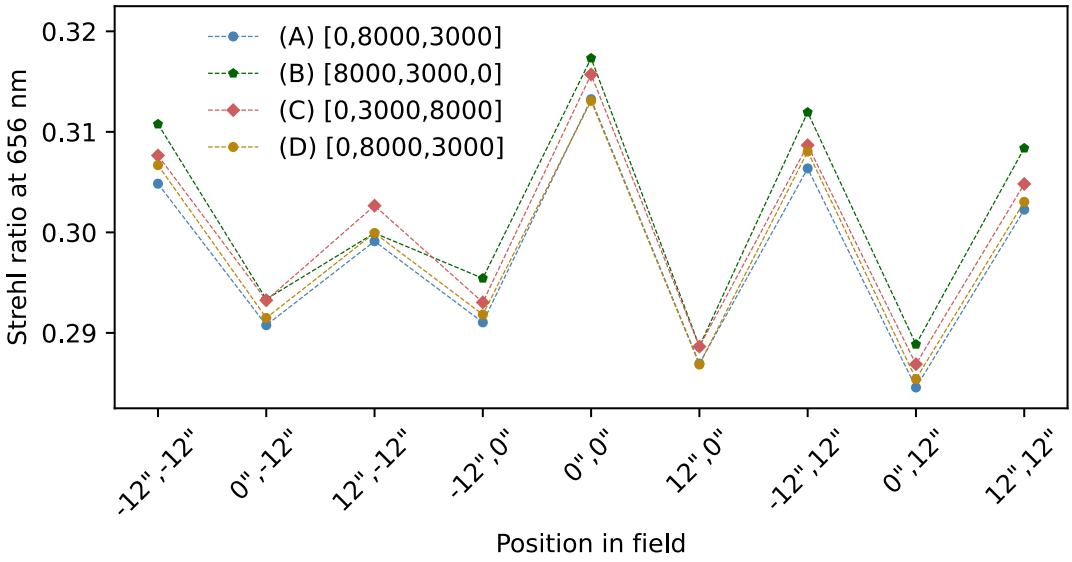

Figure 2: Strehl ratio at 656 nm as a function of position in the science field for the four different DM sequences.

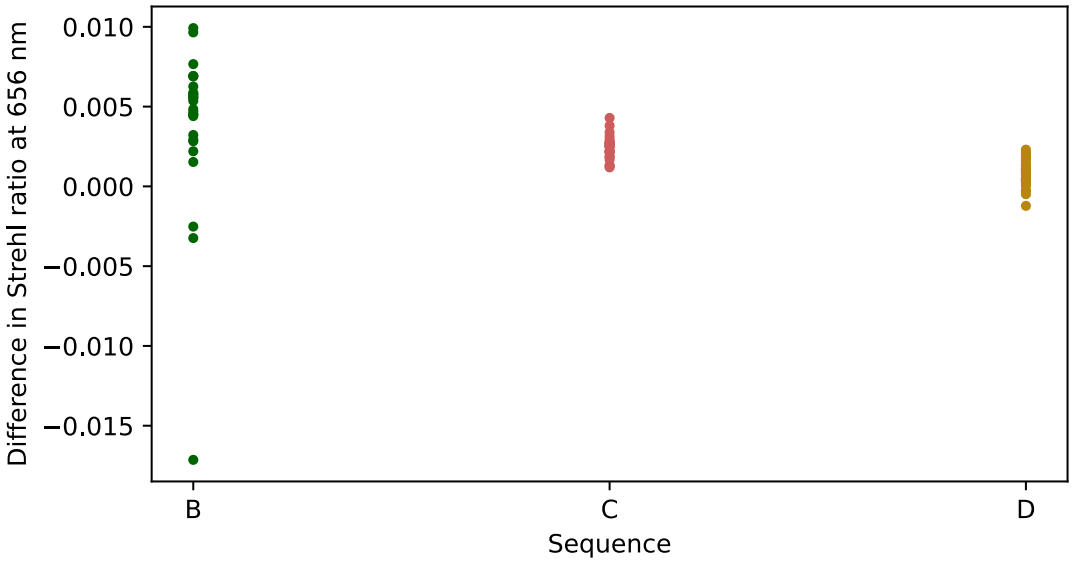

Figure 3: Difference in Strehl ratio at 656 nm between Sequences (B), (C) and (D) with respect to Sequence (A).

the results are less strongly correlated with the results of Sequence (A). The mean and standard deviation of the Strehl ratio across the field is tabulated in Table 4.

Table 4: Mean and standard deviation of the Strehl ratio at 656 nm over the science field of view.

Sequence	(A)	(B)	(C)	(D)
Strehl ratio	0.2977 ± 0.0115	0.3016 ± 0.0126	0.3001 ± 0.0117	0.2985 ± 0.0117

The comparison between Sequences (A) and (B) for the on-sky experiment is not perfectly fair because the

actuator density of the pupil plane DM used in (B) matches the WFS sampling, while the one in (A) is 10% higher. The simulations were also run with mismatched actuator densities. To make the comparison between sequences fair, the simulations were repeated using identical DMs in different order. Sequence (D) is the same as Sequence (A) except that it uses DM3 instead of DM0 as the pupil plane DM to be consistent with Sequences (B) and (C). Sequence (C) is the one recommended by Hardy,[13] Flicker,[14] and Farley *et al*[15] but produces the lowest Strehl ratio.

Sequence (B) requires the least amount of regularization of the reconstructor for a stable control loop, an important factor for on-sky operations where the seeing can change rapidly. This is probably due to the fact that there is no DM between the pupil plane DM and the WFSs to induce dynamic misregistration. Not surprisingly, Sequences (A) and (D) require the most regularization, since the DMs are not placed in order of altitude.

The simulation results are very instructive and teach us several lessons. The difference in performance between the different DM sequences is small and probably not sufficiently large to drive the design of the MCAO system. There is no advantage in placing the DMs from lowest to highest altitude, as commonly believed. In fact, placing the DMs from highest to lowest altitude, which is the order in which the layers are imaged by the telescope, produces the highest Strehl ratio, the most stable control loop and simplest post-focal optical design. Finally, the fact that Sequence (D) outperforms Sequence (A) indicates that the matching the pupil plane DM actuators to the WFS subapertures is important.

4. SIMULATIONS OF THE MAVIS MCAO SYSTEM

MAVIS (MCAO Assisted Visible Imager and Spectrograph) is an MCAO instrument under design for the VLT. It aims to provide a $30''\times30''$ corrected field of view at an angular resolution close to the diffraction limit at visible wavelengths. MAVIS takes advantage of the already existing Adaptive Optics Facility, which includes an Adaptive Secondary Mirror (ASM) and sodium laser guide stars (LGSs). It senses the wavefront using a constellation of 8 LGSs supplemented by tip-tilt measurements from up to 3 NGSs.[10, 23, 24] The simulation conditions are the nominal operating conditions for which MAVIS is designed.

4.1 Simulation parameters

The Very Large Telescope is modeled using 480 pixels across a circular pupil with a diameter of 8.0 m, with a central obscuration of 1.28 m. The zenith angle is 30° with an r_0 at 500 nm of 0.129 m at zenith. Other atmospheric parameters are tabulated in Table 5.

Table 5: Turbulence profile used in the simulations of the MAVIS MCAO system.

Elevation (m)	30	140	281	562	1125	2250	4500	7750	1100	14000
C_n^2 ($\times10^{-14}\mathrm{m}^{1/3}$)	26.81	0.91	1.82	2.72	0.45	2.72	4.09	1.81	2.27	2.27
Turbulence fraction	0.59	0.02	0.04	0.06	0.01	0.05	0.09	0.04	0.05	0.05
Wind speed ($\mathrm{m\,s}^{-1}$)	6.6	5.9	5.1	4.5	5.1	8.3	16.3	30.2	34.3	17.5
Wind direction (°)	66	29	17	350	270	190	78	12	221	16

PropAO cannot yet handle LGSs. Instead, we simulate the LGSs as being bright NGSs (noiseless point sources at infinity). There are eight WFSs in a regular octagon at a distance of $17.5''$ from the optical axis. The wavefront sensing parameters are tabulated in Table 6. The wavelength of 1000 nm was required in order to ensure that the field of view of the detector is sufficiently large without increasing the sampling of the pupil.

Table 6: Wavefront sensing parameters.

Wavelength	1000 nm
Subapertures across pupil	40
Subaperture size	0.2 m

Even though the adaptive secondary mirror (ASM) will be used, the three DMs are modeled as having a regular grid of actuators with a super Gaussian influence function,[22] Some of the value used in the simulations, shown in Table 7, do not correspond exactly to the system under design.

Table 7: Deformable mirror parameters used to simulate the MAVIS MCAO system.

DM	0	1	2
Altitude	0 m	6000 m	13 500 m
Actuators	27×27	32×32	25×25
Actuator pitch	300 mm	300 mm	450 mm

The interactuator spacing for DM0 and DM1 matches the size of the WFS subapertures, with the location of the actuators in the corner of the subapertures.

The following DM sequences were compared in simulation:

(A): DM0, DM1, DM2 at 0 m, 6000 m and 13 500 m

(B): DM2, DM1, DM0 at 13 500 m, 6000 m and 0 m

(C): DM0, DM2, DM1 at 0 m, 13 500 m and 6000 m

Sequence (A) has the layers from lowest to highest altitude, while Sequence (B) has the DMs from highest to lowest altitude. Sequence (C) corresponds to the case where an adaptive secondary mirror is conjugate to the pupil plane and the remaining DMs are sequenced in the order in which they are imaged by the telescope, which is the actual configuration of MAVIS.

The reconstructor was a regularized least-squares reconstructor[22] operating with pseudo open-loop control with a loop gain of 0.4. The frame rate was 1000 Hz with a loop delay of one cycle. Each simulation consists of a total of 5000 iterations for an integration time of 5 s, and three sets of simulations were run for each sequence with different phase screens. The Strehl ratio was evaluated at the same locations as the WFS but at a wavelength of 550 nm.

4.2 Simulation results

The Strehl ratio was evaluated at nine different positions in the field corresponding to one quadrant of the MAVIS science field of view. The simulated average Strehl ratio as a function of position in the field is plotted in Figure 4. The results are consistent with the output of simulations using PASSATA. The performance of the three DM sequences is similar, with the actual MAVIS configuration providing the best performance. For the turbulence strength and interactuator spacing simulated, the dynamic misregistration was not an issue, so placing the pupil plane DM last provides no benefit.

The simulations run fast. Each iteration of the control loop, including the WFSs, takes 226 ms, while computing all nine the PSFs takes another 241 ms on a laptop equipped with an NVIDIA RTX A5000 GPU.

5. CONCLUSION

The DM sequence for astronomical MCAO systems has long been a vexing issue. Previously, some theoretical considerations that applied wavefront compensation using geometric optics as well as numerical calculations of scintillation effects suggested that the best performing sequence of DMs is from lowest altitude to highest altitude. However, this is not borne out in practice. On-sky tests on Clear and the simulations presented here suggest that solar MCAO systems benefit from having the pupil plane DM last rather than first. This can be explained by the fact that placing DMs between the pupil plane DM and the WFSs leads to dynamic misregistrations between the pupil plane DM (which corrects the bulk of the turbulence) and the WFSs. We recommend that solar DMs sequence the DMs from highest to lowest altitude if possible, because this leads to better performance as well as increased loop stability in poor seeing or at low elevations.

For MAVIS, the proposed configuration, which uses an ASM followed by two DMs from highest to lowest altitude, produced the best performance in simulations. However, the difference in the performance between the sequences is small. The sequence with the simplest or best performing optical design should be preferred, and the inclusion of relay optics in order to reimage the pupils is not warranted.

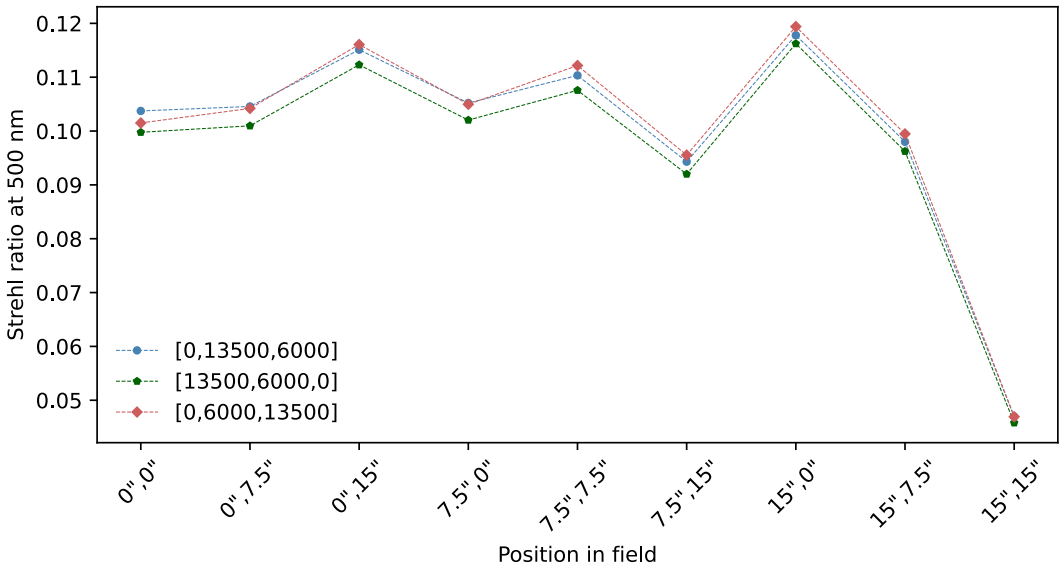

Figure 4: Strehl ratio at 550 nm as a function of position in the science field for the three different DM sequences.

Finally, this work demonstrates that it is now computationally feasible to include Fresnel propagation in simulations of MCAO systems (especially using GPUs) and the PROPER Optical Propagation library makes it straight-forward to implement.

Acknowledgments

This work was supported by the EST Project Office, funded by the Canary Island Government (file SD 17/01) under a direct grant awarded to EST on grounds of public interest. We would like to thank John Krist (JPL) for advice on the use of PROPER and Rodolphe Conan (GMT) for the suggestion to use the CuPY library in place of the NumPY library.

REFERENCES

[1] F. Rigaut and B. Neichel, "Multiconjugate adaptive optics for astronomy," *Annual Review of Astronomy and Astrophysics* **56**, 277–314 (2018).

[2] E. Marchetti, N. N. Hubin, E. Fedrigo, *et al.*, "MAD: the ESO multiconjugate adaptive optics demonstrator," in *Adaptive Optical System Technologies II*, **4839**, 317–328, International Society for Optics and Photonics (2003).

[3] F. Rigaut, B. Neichel, M. Boccas, *et al.*, "Gemini multiconjugate adaptive optics system review–I. Design, trade-offs and integration," *Monthly Notices of the Royal Astronomical Society* **437**(3), 2361–2375 (2014).

[4] B. Neichel, F. Rigaut, F. Vidal, *et al.*, "Gemini multiconjugate adaptive optics system review–II. Commissioning, operation and overall performance," *Monthly Notices of the Royal Astronomical Society* **440**(2), 1002–1019 (2014).

[5] K. K. R. Santhakumari, C. Arcidiacono, M. Bergomi, *et al.*, "LINC-NIRVANA Commissioning at the Large Binocular Telescope–Lessons Learned," *arXiv preprint arXiv:2112.01262* (2021).

[6] T. Berkefeld, D. Soltau, and O. von der Lühe, "Results of the multi-conjugate adaptive optics system at the German solar telescope, Tenerife," in *Astronomical Adaptive Optics Systems and Applications II*, **5903**, 59030O, International Society for Optics and Photonics (2005).

[7] T. Berkefeld, D. Soltau, and O. von der Lühe, "Multi-conjugate solar adaptive optics with the VTT and GREGOR," in *Advances in Adaptive Optics II*, **6272**, 627205, International Society for Optics and Photonics (2006).

[8] T. Rimmele, S. Hegwer, J. Marino, *et al.*, "Solar multi-conjugate adaptive optics at the Dunn Solar Telescope," in *1st AO4ELT Conference-Adaptive Optics for Extremely Large Telescopes*, 08002, EDP Sciences (2010).

[9] D. Schmidt, N. Gorceix, P. R. Goode, *et al.*, "Clear widens the field for observations of the Sun with multi-conjugate adaptive optics," *Astronomy & Astrophysics* **597**, L8 (2017).

[10] F. Rigaut, R. McDermid, G. Cresci, *et al.*, "MAVIS conceptual design," in *Ground-based and Airborne Instrumentation for Astronomy VIII*, **11447**, 378–393, SPIE (2020).

[11] D. Schmidt, A. Beard, A. Ferayorni, *et al.*, "On the upgrade path to GLAO and MCAO on the Daniel K. Inouye Solar Telescope," in *Adaptive Optics Systems VIII*, **12185**, 208–220, SPIE (2022).

[12] T. Berkefeld, "Status of the preparatory work for the 4m European Solar Telescope," in *Adaptive Optics Systems VI*, **10703**, 1070315, International Society for Optics and Photonics (2018).

[13] J. W. Hardy, *Adaptive optics for astronomical telescopes*, Oxford University Press (1998).

[14] R. C. Flicker, "Sequence of phase correction in multiconjugate adaptive optics," *Optics Letters* **26**(22), 1743–1745 (2001).

[15] O. Farley, J. Osborn, T. Morris, *et al.*, "Deformable mirror configuration in MCAO: is propagation a fundamental limit on visible wavelength correction?," *AO4ELT5* (2017).

[16] D. Schmidt, N. Gorceix, and P. Goode, "On the sequence of deformable mirrors in MCAO: findings from an on-sky, closed-loop experiment," in *Adaptive Optics Systems VII*, **11448**, 1144842, International Society for Optics and Photonics (2020).

[17] M. A. van Dam, B. Femenía Castellá, Y. Martín Hernando, *et al.*, "Scintillation effects and the optimal sequence of deformable mirrors in multi-conjugate adaptive optics," *Journal of Astronomical Telescopes, Instruments, and Systems* **7**(4), 049002–049002 (2021).

[18] J. E. Krist, "PROPER: an optical propagation library for IDL," in *Optical Modeling and Performance Predictions III*, **6675**, 66750P, International Society for Optics and Photonics (2007).

[19] D. Schmidt, T. Berkefeld, B. Feger, *et al.*, "Latest achievements of the MCAO testbed for the GREGOR Solar Telescope," in *Adaptive Optics Systems II*, **7736**, 773607, International Society for Optics and Photonics (2010).

[20] M. A. van Dam, Y. M. Hernando, M. N. Cagigal, *et al.*, "Overcoming the effect of pupil distortion in multiconjugate adaptive optics," in *Adaptive Optics Systems VII*, **11448**, 114480P, International Society for Optics and Photonics (2020).

[21] D. L. Fried, "Least-square fitting a wave-front distortion estimate to an array of phase-difference measurements," *JOSA* **67**(3), 370–375 (1977).

[22] M. A. van Dam, D. Le Mignant, and B. A. Macintosh, "Performance of the Keck Observatory adaptive-optics system," *Applied Optics* **43**(29), 5458–5467 (2004).

[23] D. Greggio, B. Taylor, M. Bonaglia, *et al.*, "MAVIS adaptive optics module: optical configuration and expected performance," in *Adaptive Optics Systems VIII*, **12185**, 2088–2100, SPIE (2022).

[24] V. Viotto, E. Pinna, G. Agapito, *et al.*, "MAVIS: preliminary design of the adaptive optics module," in *Adaptive Optics Systems VIII*, **12185**, 623–634, SPIE (2022).